Organic Process Research & Development

ARTICLE

pubs.acs.org/OPRD

Heat Pipe-Mediated Control of Fast and Highly Exothermal Reactions

N. Ehm[†] and H. Löwe[*,†,‡]

[†]Johannes Gutenberg University Mainz, 55128 Mainz, Germany

[‡]Institut fuer Mikrotechnik Mainz GmbH, 55129 Mainz, Germany

ABSTRACT: The synthesis of 1-ethyl-3-methylimidazolium ethyl-sulfate ([EMIM]$EtSO_4$) from 1-methyl-imidazole and diethyl sulfate suffers from highly exothermal behavior. Once the activation energy barrier is reached (E_A = 89 kJ mol^{-1}), the bimolecular reaction accelerates with a high reaction enthalpy (ΔH = −130 kJ mol^{-1}).[1−3] The excess of heat has to be concurrently dissipated to avoid hot spots or thermal runaways. Depending on the volume flow velocity of the reactants and the applied reactor temperature, the reaction zone can be shifted inside the reactor from the inlet to the outlet and vice versa. Therefore, a sophisticated thermal control, oscillating between providing activation energy and intense cooling of the reaction mixture, is required. Heat pipes intrinsically allow both fast dynamic bidirectional heating and cooling. A stainless steel chiplike setup equipped with an externally heated, modified heat pipe system was used.[4] Independently from the reactant volume flow, a colorless and ^{1}H NMR clean product could be obtained by setting a self-controlled optimal operating temperature of about 100 °C.

INTRODUCTION

In the last two decades, the advantages of micro-structured reactors compared to conventional batch technologies was successfully demonstrated.[5] Most of the established processes carried out in batches are presenting several technical disadvantages. In some cases, reactions are running below their kinetic limits.[6,7] This problem can be omitted not only by simple transfer to microflow conditions but also by applying sophisticated heating or cooling procedures as well as by mixing at a much faster rate compared to the reaction rate.[8−10] Thus, the specific heat transfer coefficient in microscale setups is much higher than for conventional heat exchangers. Moreover, impaired heat release and thermal overshooting can be avoided.[11−13] The synthesis of [EMIM]$EtSO_4$ was intensively investigated in both batch and microflow conditions. Promising procedures, e.g. the use of microreactors combined with subsequent heat/cool zones,[14,15] or spray techniques with a cosolvent,[16] were used to avoid hot spots and thermal runaways. Recently, we proofed the efficiency of heat pipes for cooling a similar highly exothermal reaction.[4] Heat pipes can be used not only for cooling but also for heating at the same time because of the bidirectional heat flux inside of the heat pipe tube.[17−20] The synthesis of [EMIM]$EtSO_4$ was investigated in a thermal, isolated, single-channel microreactor equipped with three heat pipes under continuous flow conditions. At room temperature, the reaction has a latency period (delay time until the reaction starts) of about 20 s. Thus, the reaction takes place uncontrolled outside in the withdrawal channel or even in the receiving vessel. In the worst case, the reaction mixture bursts out. By applying activation energy from instantaneous heating via heat pipes, the reaction takes place immediately and can be shifted from the receiving vessel back into the reactor. Due to the bidirectional heating and cooling behavior of the applied heat pipes, the optimal operating temperature can be precisely adjusted independently from a wide range of volume flow rates.[4] As a result, the final product appears as a colorless liquid, indicating the absence of hot spots and uncontrolled overheating.

EXPERIMENTAL SECTION

The major interest in this work is the formation of 1-ethyl-3-methylimidazoliumethylsulfate (**3**) from 1-methylimidazole (**1**) and diethyl sulfate (**2**):

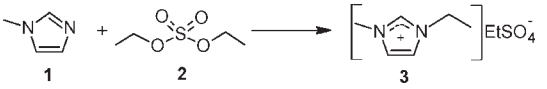

1 **2** **3**

1-Methylimidazole (**1**) (99%) was purchased from Carl Roth and further purified by short path distillation (UIC GmbH, Alzenau). Diethyl sulfate (**2**) (99%) was delivered from Acros Organics and used without further purification. No further solvents were used.

The experimental setup consists, as previously described,[4] of a micro-structured reactor plate (Figure 1),mounted on an adapted heat pipe, HPLC pumps (Knauer, HPLC-Pump K-1800, 1000-mL pump heads), and a PC-supported temperature data logger. Initial flow rates were respectively set to $\dot{V}$ = 0.3 mL min^{-1} for (**1**) and $\dot{V}$ = 0.5 mL min^{-1} for **2**, corresponding to a molar flow rate of $\dot{n}$ = 3.8 × 10^{-3} mol min^{-1}.

The cooling/heating system is composed of three commercially available heat pipes commonly used as tuning equipment from PC shops (e.g., Thermaltake Technology Co., Ltd., Taiwan; Quick-Ohm Küpper & Co. GmbH, Germany). The heat pipes are interposed in the heat sink plate, which is screwed and pressed on the reactor surface, while the opposite ends of the heat pipes are connected to an array of parallel oriented air cooling fins (Figure 2). The required activation energy is obtained from an external heat source (hot air stream). The hot air stream was directed longitudinally to the cooling fins.

Type K thermocouples (TC Mess- and Regelungstechnik GmbH, Mönchengladbach) connected to a Squirrel data logger

Special Issue: Safety of Chemical Processes 11

Received: August 9, 2011
Published: September 22, 2011

(2020/2040 series, Grant Instruments, Cambrige, England) were used to record temperature measurements series (see Figure 3). Sets of temperature measurements were made at the heating zone of the external heat source (hot air stream) (◊), between the cooling fins (●), and on the heat sink area surface (○). The temperatures inside the reaction channels (♦ and ×) were not directly accessible. Therefore, the thermocouples were inserted into longitudinal milled grooves in the peek cover. A graphite seal, placed between peek cover and reaction plate, avoids direct contact with the reaction fluid and defines a close proximity between thermocouples and reaction channels.

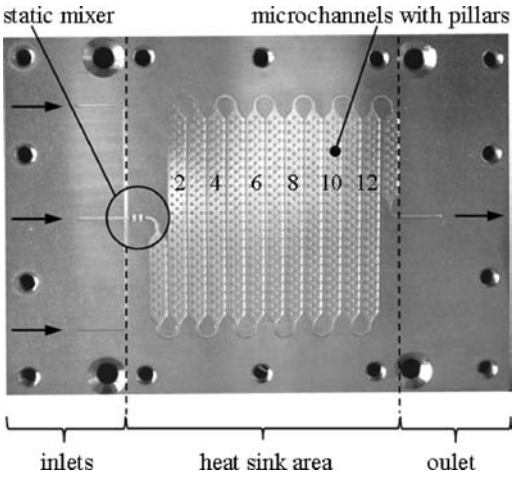

Figure 1. Single-channel micro-structured reactor plate made of stainless steel with integrated static mixer.[4] Channel length 425 mm, volume 290 μL, channel surface area 970 mm^2.

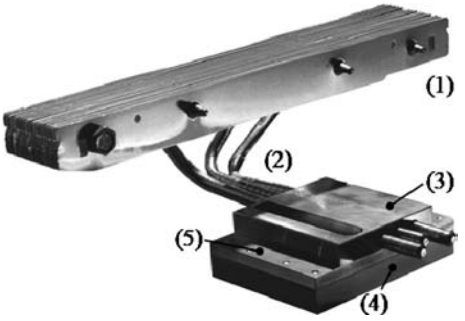

Figure 2. Microreactor equipped with a heat pipe cooling system. (1) Aluminum fins connected to the heat pipes, (2) three independent heat pipes, (3) heat sink, (4) PEEK cover, (5) micro-structured reactor plate.

It should be considered that the measured temperatures in the channels are a few degrees different from the real temperatures. Nevertheless, temperature differences caused by shifting the reaction zone inside the reactor between two different channels (channels 4 and 12) could be easily observed. Other temperature measuring points are directly placed in the withdrawal channel (■) and in the receiving vessel (▲). An overflow vessel ensures a defined volume of 3 mL, which allows a constant temperature measurement. Without overflow, the measured temperatures significantly become lower due to the mixing with already collected and cooled-down product.

RESULTS AND DISCUSSION

The dependency of reaction heat and flow rates is shown in Figure 4. Below 50 °C operating temperatures (time period A), the reaction takes place uncontrolled out of the reactor, in the receiving vessel. In the worst case, the reaction bursts out by thermal overshooting (160 °C outlet temperature), resulting in the formation of a dark-yellow product. At higher operating temperatures, the reaction shifts from the receiving vessel back into the microreactor. The time period (B) demonstrates the typical temperature profile of the preheating process by the above-mentioned heat pipe system. The outlet temperature immediately decreases by increasing the operating temperature. In section (C), the flow rate was doubled (1.6 mL min^{-1}). Whereas the reaction temperature increases, the operating temperature (temperature measured at the reactor surface)

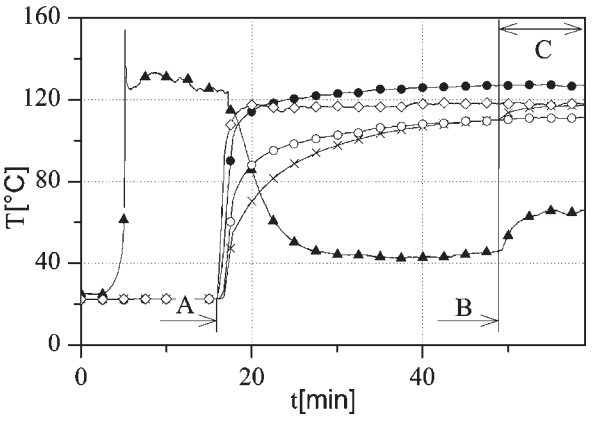

Figure 4. Temperature curves of the preheating process and demonstration of independency of flow rate. (▲) Receiving vessel, (×) channel 4, (●) cooling fins, (○) operating temperature (implies the temperature on the reactor surface), (◊) external heat source.

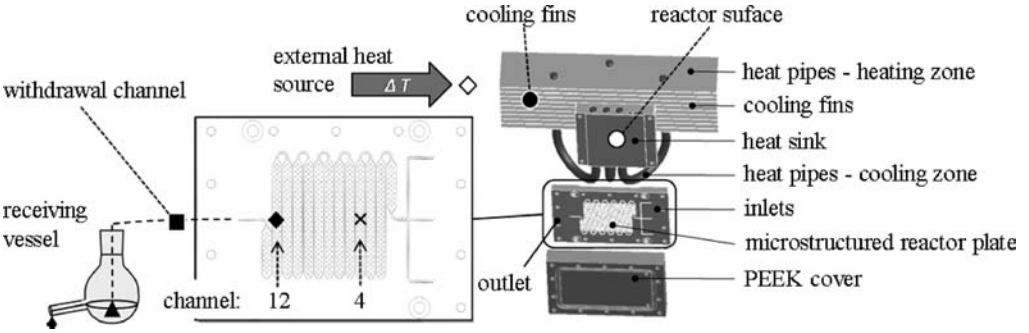

Figure 3. Temperature measuring spots for the temperature curves are marked.

dx.doi.org/10.1021/op200216y |*Org. Process Res. Dev.* 2011, 15, 1438–1441

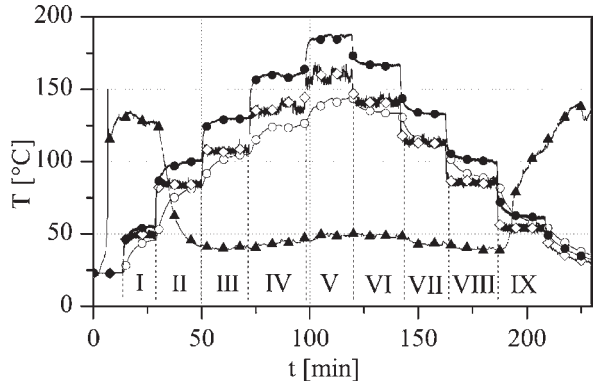

Figure 5. Temperature-controlled reaction. The reactor was heated and cooled down again stepwise. (▲) Receiving vessel, (◊) external heat source, (●) cooling fins, (○) operating temperature (implies the temperature on the reactor surface).

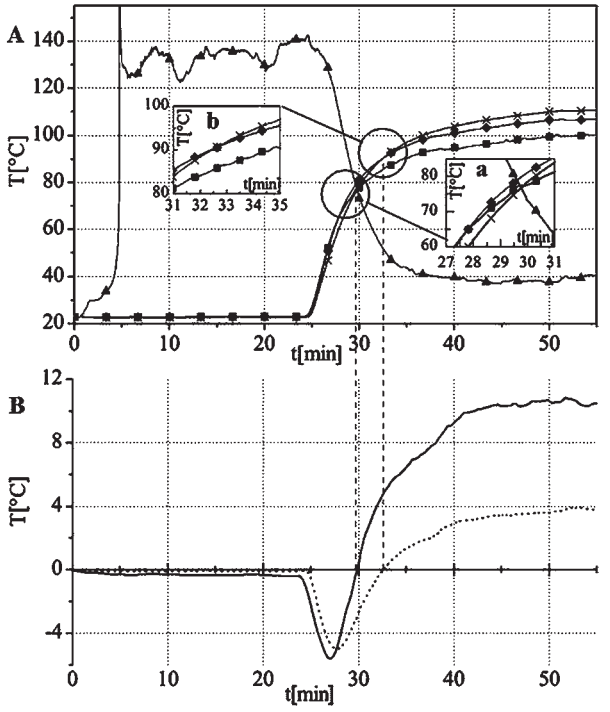

Figure 6. Reaction shift from the collecting basin into the microreactor. Plot A: (▲) receiving vessel, (♦) channel 12, (■) withdrawal channel, (×) channel 4. Plot B: temperature difference between channel 4/channel 12 (---) and channel 4/withdrawal (—) channel.

stays nearly at the same level. This is in accordance with previously published results for a similar reaction.[4] Moreover, by understanding the dynamic cooling and heating behavior of heat pipes, it is clear that at the beginning of heating, the temperature of the external heat source is higher than the temperature in the cooling fins. Once the exothermal reaction starts, the heat pipes conduct the heat to the cooling fins. As a consequence, the temperature in the cooling fins becomes higher than the temperature of the external heat source. In other words, the external heat source acts, in this case, as a cooling air flow and keeps the reactor temperature nearly on a constant level.

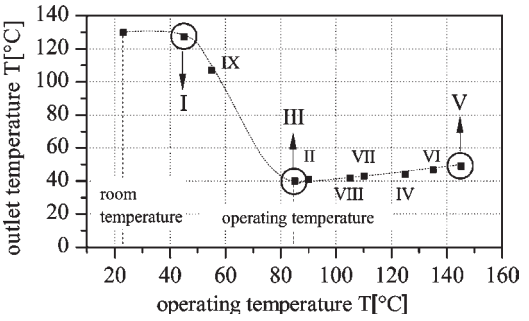

Figure 7. Determination of the optimal operating temperature. (^{1}H NMR analysis from marked data I, III, and V see Figure 8, the marked points (I–IX) are selected sections, which can also be found in Figure 5).

With this experimental setup, a fast change of the operating temperature is possible, approximately with a rate of 1 K s^{-1}. Hence, heating and heat-dissipation processes are reversible and easily reproducible (see Figures 4 and 5).

Furthermore, the reaction shift can exactly pursue from the receiving vessel into the reactor. Hence, a determination of the reaction front was possible by temperature measurements. By increasing the temperature in the reactor, reaction time is shortened and the reaction can entirely take place in the reactor, instead of partly taking place outside the channel or in the receiving vessel. As shown in Figure 6, temperatures in channels 4 and 12, the withdrawal channel, and the receiving vessel are plotted. This explains how the reaction front oscillates between the four mentioned measurement points by changing the temperature of the external heat source:

- During the heating period, the receiving vessel temperature rapidly decreases and sustains a constant temperature of approximately 40 °C. There are also intersections between the temperature curve of the withdrawal channel with channel 12 and afterwards channel 4 (Figure 6 A, a). From this point, the temperature in the withdrawal channel is the lowest, apart from the temperature in the receiving vessel. Thus, the reaction front is localized near the outlet of the reactor plate.
- Furthermore, the temperature in channel 4 exceeds the temperature in channel 12 (Figure 6 A, b). This is due to a shift of the reaction near the inlet of the microreactor.

In order to show the temperature differences between channels 4 and 12 and the reactor outlet, they are plotted as function of time in Figure 6 B. Hence, the reaction shift is visualized. The dotted line shows the temperature difference between channel 4 and 12, while the solid line represents the temperature difference between channel 4 and withdrawal channel, respectively. At the beginning of the heating process (time 25 min), temperature differences occur. The minimum of both plotted curves reveal their maximum temperature differences. Changing of sign (Figure 6 B) indicates the points of intersections of the measured temperatures (compare Figure 6 A). Both plots converge with a constant temperature difference, once the heating process is complete. The measured temperature difference between channel 4 and the withdrawal channel is remarkably higher compared to the measured temperature difference between channel 4 and 12. This also indicates a shift of the reaction front closer to the inlet of the reactor rather than the withdrawal channel.

dx.doi.org/10.1021/op200216y |*Org. Process Res. Dev.* 2011, 15, 1438–1441

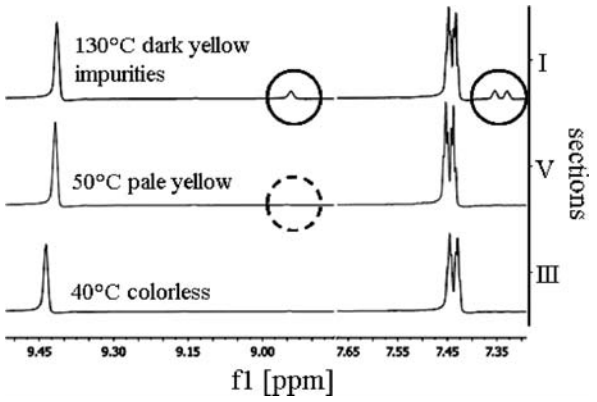

Figure 8. Byproduct caused by uncontrolled reaction outside the reactor. Discoloration appears above the optimal operating temperature (compare Figures 5 and 7). The circles mark the signals assigned the colorized side product (the dotted-line circle draws the attention to small signals, indicating very small concentrations). Full data: ^{1}H NMR (400 MHz, $CDCl_3$): δ (ppm) = 9.45 (s, 1H), 7.46 (d, J = 6.3 Hz, 2H), 4.29 (q, J = 7.3 Hz, 2H), 4.07 (q, J = 7.1 Hz, 2H), 3.98 (s, 3H), 1.52 (t, J = 7.3 Hz, 3H), 1.25 (t, J = 7.1 Hz, 3H).

The optimal operating temperature is indicated as a minimum by plotting the temperature in the receiving vessel as a function of the operating temperature (temperature of the reactor surface) as shown in Figure 7.

By performing the reaction at an optimized operating temperature, best quality and discoloration of product has been achieved. Thus, the color of the product changes from dark to pale yellow (section (I) in Figure 7 and 8) by increasing the operating temperature to the optimum at which it is colorless (85 °C, section (III) in Figure.7 and 8). However, in the range of 85 to 150 °C operating temperature (implies an outlet temperature of 40 to 50 °C, (section (V) in Figure.7 and 8)) the color of the product turns to very pale yellow again, but no byproducts could be identified by ^{1}H NMR spectroscopy. Further coloration of the product is observed above an optimal operating temperature, indicating thermal overshooting (hot spots) inside the reaction channel.

SUMMARY

Cooling of micro-structured reactors with heat pipes is not the sole conceivable application. They also can be simultaneously used as regulating systems for heating and cooling. For the investigated reaction, activation energy is required to start the high exothermal reaction. After the reaction self-accelerates in a second-order kinetic with a high and instantaneous heat release, the excess of heat has to be dissipated. The use of heat pipes offers an interesting alternative in order to rapidly heat and cool the system. Moreover, such fast temperature changes cannot be quenched by conventional driven fluidic heat exchangers, due to their tardy cooling and heating behavior. In comparison, heat pipes used in the above-described setup are able to provide and dissipate heat in a matter of seconds, due to a heat transport close to sonic velocity.[21] Optimal operating temperatures can be stabilized and easily varied by self-mediation of a properly adjusted heat pipe system.

With the above described reaction conditions and the optimized operating temperature, a lab-scale production rate of about 54 g h^{-1} (**3**) (3.8 mmol min^{-1}) is possible. Furthermore, the dissipated amount of heat equates to a performance of less than 3 W by the applied volume flow. A single conventional heat pipe, used in the setup, has a performance of approximately 60 W. Thus, the applied setup is by far oversized, and it is conceivable to run the process with much higher flow rates.[4] To enhance the application of heat pipes for microscaled reactors, βdownsized heat pipes should be used in the future.[22−24]

AUTHOR INFORMATION

Corresponding Author
loewe@uni-mainz.de.

REFERENCES

(1) Große Böwing, A.; Jess, A.; Wasserscheid, P. *Chem. Ing. Tech.* **2005**, *77*, 1430–1439.
(2) Große Böwing, A.; Jess, A. *Chem. Eng. Sci.* **2007**, *62*, 1760–1769.
(3) Minnich, C. B.; Küpper, L.; Liauw, M. A.; Greiner, L. *Catal. Today* **2008**, *126*, 191–195.
(4) Löwe, H.; Axinte, R. D.; Breuch, D.; Hang, T.; Hofmann, C. *Chem. Eng. Technol.* **2010**, *33*, 1153–1158.
(5) Wiles, C.; Watts, P. *Micro Reaction Technology in Organic Synthesis*, 1st ed.; CRC Press, Taylor & Francis Group: Boca Raton, FL, U.S.A., 2011.
(6) Schwalbe, T.; Autze, V.; Wille, G. *Chimia* **2002**, *56*, 636–646.
(7) Schwalbe, T.; Kursawe, A.; Sommer, J. *Chem. Eng. Technol.* **2005**, *28*, 408–419.
(8) Jähnisch, K.; Hessel, V.; Löwe, H.; Baerns, M. *Angew. Chem., Int. Ed.* **2004**, *43*, 406–446.
(9) Yoshida, J.-I. *Flash Chemistry - Fast Organic Synthesis in Microsystems*; Wiley-VCH: Weinheim, 2008.
(10) Yoshida, J.-I.; Nagaki, A.; Yamada, T. *Chem. Eur. J.* **2008**, *14*, 7450–7459.
(11) Yu, W.; Desmulliez, M. P. Y.; Drufke, A.; Leonard, M.; Dhariwal, R. S.; Flynn, D.; Bognar, G.; Poppe, A.; Horvath, G.; Kohari, Z.; Rencz, M. *J. Micromech. Microeng.* **2010**, *20*, 025004.
(12) Sreenath, K.; Pushpavanam, S. *Chem. Eng. J.* **2009**, *155*, 312–319.
(13) Yang, X. F.; Liu, Z.-H.; Zhao, J. *J. Micromech. Microeng.* **2008**, *18*, 035038.
(14) Löb, P.; Hessel, V.; Krtschil, U.; Löwe, H. *Chim. Oggi - Chem. Today* **2006**, *24*, 46–50.
(15) Renken, A.; Hessel, V.; Löb, P.; Miszczuk, R.; Uerdingen, M.; Kiwi-Minsker, L. *Chem. Eng. Process.* **2007**, *46*, 840–845.
(16) Löwe, H.; Axinte, R. D.; Breuch, D.; Hofmann, C.; Petersen, J. H.; Pommersheim, R.; Wang, A. *Chem. Eng. J.* **2010**, *163*, 429–437.
(17) Pruschek, R.; Schindler, M.; Moritz, K. *Chem. Ing. Tech.* **1967**, *39*, 21–26.
(18) Zimmermann, P. *Forsch. Ingenieurwes. (Springer)* **1971**, *37*, 44–47.
(19) Dunn, P. D.; Reay, D. A. *Phys. Technol.* **1973**, *4*, 187–201.
(20) Reay, D. A.; Kew, P. A. *Heat Pipes*; 5th ed.; Elsevier Ltd.: Amsterdam, 2006.
(21) Faghri, A. *Heat Pipe Science and Technology*; 1st ed.; Taylor & Francis; , 1995.
(22) Suh, J.-S.; Park, Y. S. *Tamkang J. Sci. Eng. (Korean)* **2003**, *6*, 201–206.
(23) Mahmood, S. L.; Akhanda, M. A. R. *J. Therm. Sci.* **2008**, *17*, 247–252.
(24) Shukla, K. N. *J. Electron. Packag.* **2009**, *131*, 024502 3 pages.